GEOLOGY | THE GEOLOGICAL SOCIETY OF AMERICA®

https://doi.org/10.1130/G45512.1

Manuscript received 21 August 2018
Revised manuscript received 22 November 2018
Manuscript accepted 10 December 2018

Published online 18 January 2019

Fracture healing and strength recovery in magmatic liquids

A. Lamur[1]*, J.E. Kendrick[1], F.B. Wadsworth[1,2], and Y. Lavallée[1]
[1]Department of Earth, Ocean and Ecological Sciences, University of Liverpool, Liverpool L69 3GP, UK
[2]Department of Earth Sciences, Durham University, Durham DH1 3LE, UK

ABSTRACT

Cycles of fracture and healing in magma are important controls on outgassing time scales and repetitive seismicity at silicic volcanoes. Here, we experimentally drove silicate melts (at 10^9–10^{11} Pa·s) to tensile failure, measuring the strength during fracture of the otherwise liquid material. We then took the same melts with parallel contact surfaces and closed the fracture under compressive stress and recorded the evolution of tensile strength of the interface healed for different times. We provide a semi-empirical model for fracture healing time scales useful for volcanic applications. As the time available for healing is increased, strength nonlinearly recovers toward that of unfractured glass. We parameterized the healing kinetics as a three-stage process: (1) relaxation of the compressive stress, (2) fracture surface–surface wetting, and (3) diffusive removal of the interface. During welding of these surfaces in air, we observed that micropores are trapped along the fracture plane, which may inhibit complete healing and provide a textural record of relict fracture planes in volcanic glasses. We conclude that at magmatic conditions, fracture healing is efficient in crystal-poor melts, and it could rapidly seal outgassing pathways over eruptive time scales, contributing to cyclic behavior associated with recurring gas-and-ash explosions and outgassing events.

INTRODUCTION

In shallow volcanic conduits, ascending magmas can undergo multiple fracture and healing cycles (Tuffen et al., 2003), producing diagnostic relict fracture textures (Goto, 1999; Tuffen and Dingwell, 2005) thought to contribute to outgassing (e.g., Castro et al., 2012) and minor gas-and-ash venting episodes (e.g., Kendrick et al., 2016), which may generate low-frequency seismic signals prior to large eruptions (Neuberg et al., 2006). Despite being important for interpreting geophysical and geochemical signals at active silicic volcanoes, the strength recovery of planar fractures has not been constrained, and studies have instead focused on how diffusive exchange of volatiles occurs across the fracture interface (e.g., Yoshimura and Nakamura, 2010). In both volcanic and tectonic settings, trails of microbubbles and microlites in flow bands, or fragments and glass inclusions in tuffisite veins (Tuffen and Dingwell, 2005; Cabrera et al., 2011; Castro et al., 2012; Kolzenburg et al., 2012; Kendrick et al., 2016; Gardner et al., 2017) have been interpreted as relict evidence for fracture healing processes. Magmas are viscoelastic materials that readily fracture when imposed shear stresses result in strain rates that exceed the inverse of the structural relaxation time τ (Dingwell and Webb, 1989). The relaxation time τ is proportional to the viscosity η and shear modulus at infinite frequency G_∞ by $\tau = \eta/G_\infty$, where G_∞ may be approximated as 10^{10} Pa (Dingwell and Webb, 1989). Unrelaxed elastic behavior leading to failure occurs when strain rates locally exceed $10^{-2}/\tau$ (Dingwell and Webb, 1989). This strain-rate limit represents the critical transition to fractured magma, and open-system degassing (e.g., Gonnermann and Manga, 2003; Castro et al., 2012). While this critical time scale for fracturing is well constrained, the interfracture healing time scales have received comparatively less attention (Yoshimura and Nakamura, 2010). Sintering theory has been applied to healing and strength recovery of particulate material, relevant to fracture infill (e.g., Vasseur et al., 2013; Kendrick et al., 2016; Wadsworth et al., 2016), while for planar (particle-free) fractures, the healing and strength-recovery time scales are less well known. Nevertheless, Tuffen et al. (2003) proposed that magmas fracture and heal repetitively as they ascend through the crust. They suggested that healing and strength recovery might occur over times equal to the sum of a viscous period and a diffusive period. Here, we provide a framework for testing this hypothesis and a first quantitative predictive tool for scaling strength recovery in these repetitive fracture-healing processes.

MATERIALS AND METHODS

We performed fracture healing experiments on two standard borosilicate glasses with well-constrained temperature-viscosity relationships: (1) SRM 717a from the National Institute of Standards and Technology (NIST, USA), and (2) Duran® glass (Schott Duran Glass Solutions [SDGS]) from Schott (GmbH, Germany).

First, we measured the tensile strength σ_0 of each glass by direct tensile tests on dog-bone samples (ISRM, 1978) using a 5969 Instron uniaxial press with a split furnace from Severn Thermal Solutions (UK). Each sample (16 mm diameter and a total length of 160 mm, with 35 mm in the center ground to 8 mm diameter) was loaded into the mechanical grips of the press and heated up at 5 °C min^{-1} to target temperatures that provided a viscosity of 10^{10} Pa·s (560 °C for NIST and 630 °C for SDGS); the sample was thermally equilibrated over a period of 30 min, and direct pull was conducted at an axial strain rate of 10^{-1} s^{-1} (which is greater than $10^{-2}/\tau$), sufficient to ensure dominantly elastic behavior. The uncertainty on all sample temperatures was approximately 3 °C.

Fracture healing experiments were performed in air on samples in which an artificial fracture was cut through the center perpendicular to the long axis and the fracture surfaces were ground flat (Fig. DR2 in the GSA Data Repository[1]). We chose to use artificially cut fractures, rather than tensile fractures created in situ, to ensure repeatability of the results

*E-mail: anlamur@liverpool.ac.uk

[1]GSA Data Repository item 2019067, supplementary methods and raw data, is available online at http://www.geosociety.org/datarepository/2019/, or on request from editing@geosociety.org.

CITATION: Lamur, A., Kendrick, J.E., Wadsworth, F.B., and Lavallée, Y., 2019, Fracture healing and strength recovery in magmatic liquids: Geology, v. 47, p. 195–198, https://doi.org/10.1130/G45512.1

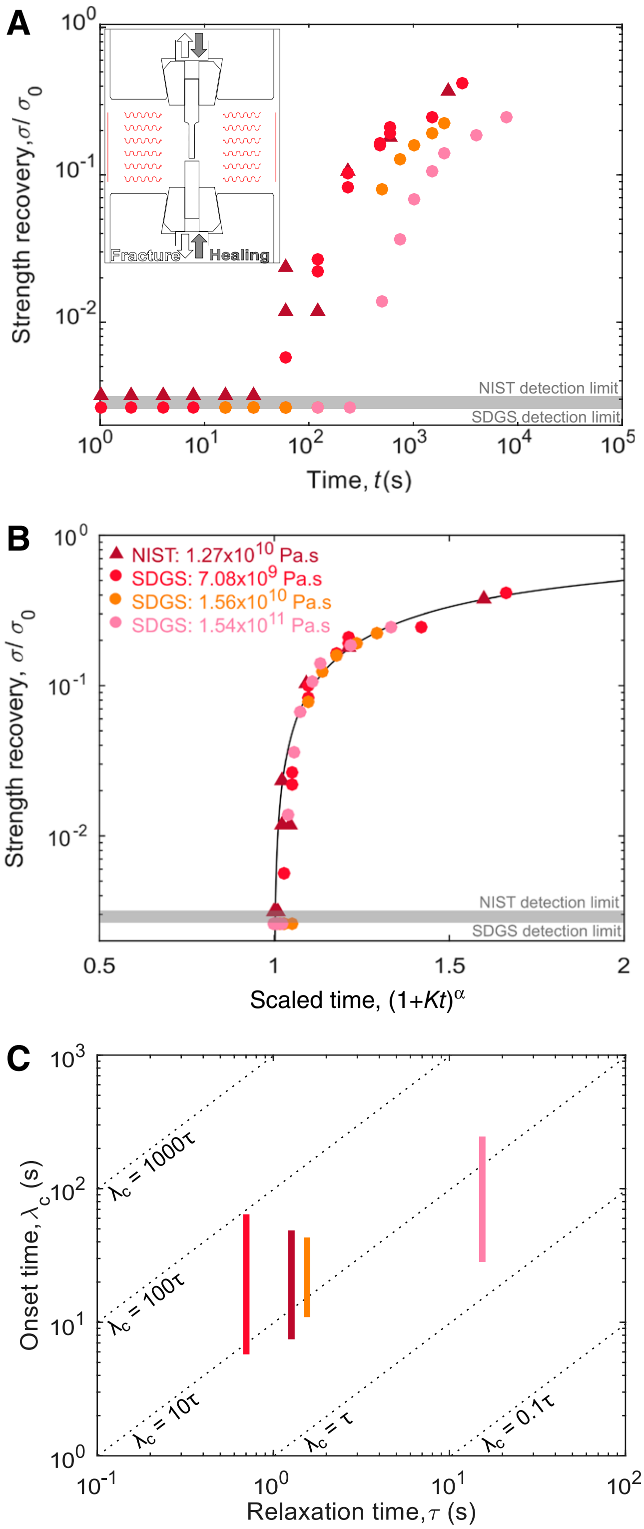

Figure 1. A: Normalized tensile strength recovered (where 1 represents tensile strength of melt measured at high temperature) as a function of contact time for experiments on NIST (U.S. National Institute of Standards and Technology; triangles) and Duran® glass (Schott Duran Glass Solutions [SDGS]; circles) melts at different viscosities. Horizontal gray bar represents detection limit range for press. Inset: Experimental setup for cyclic fracture (white arrow) and healing (gray arrow) experiments. B: Time axis normalized by fitted parameters K and α in the form of $(1 + Kt)^{\alpha}$, showing good agreement between model and data. C: Relationship between extrapolated onset time, λ_c, and relaxation time scale of glasses, τ, calculated with our model for different viscosities. Dotted lines show different $\lambda_c \propto \tau$.

using a controlled fracture geometry. The sample pair was then loaded into the mechanical grips of the press, positioned parallel and not in contact (Fig. 1A, inset), heated up to the target temperature (560 °C for NIST and 590 °C, 630 °C, or 645 °C for SDGS), providing sample viscosities between 7×10^9 and 1.5×10^{11} Pa·s (or $0.7 < \tau < 15$ s), and thermally equilibrated over a period of 30 min. After this time, the upper sample was forced into contact with the lower sample at 0.02 mm s^{-1} until an initial axial stress of between 1 and 6 MPa was reached, and the sample was held for variable experimental time scales of $0.5 < t < 8000$ s. The low stresses used were selected to ensure minimal lateral flow of the sample; the evolving contact area due to flow was monitored through a window in the furnace to correct for bulging and changes in compressive stress (Fig. DR3). After the target time, the rods were pulled apart at a constant extension rate of 3.5 mm s^{-1} to attain a strain rate of 10^{-1} s^{-1} to ensure a dominantly brittle response and to avoid viscous deformation. Here, the measured peak stress required to fracture the partially healed sample pair was measured and compared to the intact tensile strength of the melt as a measure of healing efficiency.

RESULTS AND A KINETIC MODEL FOR FRACTURE HEALING

Direct tension tests on NIST 717a and SDGS at a viscosity of 10^{10} Pa·s constrained the tensile strength σ_0 of these glasses to be 24.99 ± 0.05 MPa and 32.19 ± 0.04 MPa, respectively (Fig. DR4). Fracture healing experiments showed that strength recovery, tracked by σ/σ_0, is nonlinearly dependent on time (Fig. 1A), where σ is the strength of the partially healed fractured sample. We used a semi-empirical function that has been shown to capture strength recovery as a function of time t in polymers (Wool and O'Connor, 1981) of the sigmoidal form

$$\frac{\sigma}{\sigma_0} = 1 - \frac{1}{(1+Kt)^{\alpha}}, \tag{1}$$

where K (in s^{-1}) and α (dimensionless) are constants that we optimized using a least-squares minimization technique. The efficacy of Equation 1 at capturing the data can be seen when σ/σ_0 is plotted against $(1 + Kt)^{\alpha}$, where the global goodness of fit is $r^2 = 0.98$ (Fig. 1B). Extrapolating the result from Equation 1 down to a value of σ/σ_0 at the detection limit of the press, we can compute an effective onset time, λ_c, for fracture healing, before which the strength recovery is effectively zero. We also used the standard error computed from the residuals between Equation 1 and our data to propagate an error on λ_c (see the Data Repository). This error accounts for the mismatch between the data and the model at short times.

We interpret λ_c to be the time before which the silicate liquid is unrelaxed, such that $\lambda_c \propto \tau$. We find that, within the uncertainty on the model parameters, the onset time scales with this proportionality as $\lambda_c \approx 10\tau$ (Fig. 1C), providing a useful tool to find the critical time over which a magmatic fracture must be shut before nonzero strength will be achieved by healing. Furthermore, this implies that the applied stress will always be dissipated over times proportional to τ prior to strength recovery, confirming the hypothesis of Tuffen et al. (2003), and implying that the applied axial stress does not have a first-order effect on fracture healing within the range tested here.

To further understand the kinetics of this evolution, we can build a simplified physical picture of the operative mechanisms. During random-walk diffusion in a silicate network, the length l traveled by an element in the network is $l \sim (Dt)^{1/2}$. Wool and O'Connor (1981) demonstrated that initial diffusion is influenced by a "wetting time," during which the rough fracture surfaces establish contact. They provided an example where this wetting of surface area proceeds linearly with time—a so-called "constant rate wetting." Following their model, we propose that the product of the diffusive and wetting times controls this first part of the process, resulting in $l \sim (Dt)^{3/2}$ for initial-stage codiffusion wetting. At longer times, the surfaces are "fully wet," and there is near-complete surface area contact, meaning that only a single random-walk diffusive process is operative, with the standard result that $l \sim (Dt)^{1/2}$. Wool and O'Connor (1981) showed that the strength of a healing system is linearly dependent on the extent to which these diffusion mechanisms have occurred, such that $\sigma/\sigma_0 \propto l$. We find that this simple theoretical constraint is consistent with our data and that the power-law exponent of the early stage (wetting and diffusion) is 3/2, while the late-stage exponent (diffusive only) is 1/2 (Fig. 2).

IMPLICATIONS FOR SILICIC VOLCANIC ERUPTIONS

Fracture healing may be an important control on the mechanisms of shallow silicic eruptions (e.g., Castro et al., 2012) and flow emplacement (Cabrera et al., 2011). Extensive, connected fracture networks are a primary outgassing pathway in silicic magmas (e.g., Cabrera et al., 2011; Berlo et al., 2013; Castro et al., 2014). Furthermore, fracturing and increased gas release have been argued to be important controls on shifts in eruptive style from explosive to effusive or hybrid explosive-effusive (e.g., Edmonds et al., 2003; Gonnermann and Manga, 2003; Yoshimura and Nakamura, 2010; Cabrera et al., 2011; Castro et al., 2012). As proposed by Cabrera et al. (2011) and Castro et al. (2012, 2014), and experimentally shown by Yoshimura and Nakamura (2010), the formation of dense, silicic obsidian might result from fracture-healing cycles. Once healed, the only remaining evidence for the fracture may be trails of isolated pores that trace the remnant fracture surface, which we reproduce here in Figure 3.

Our work has shown that healing is a kinetic process controlled first by structural relaxation and second by wetting and diffusion in silicate melts. The pressure acting on a closing fracture may shorten the total longevity of the initial wetting phase, and it can also impact the solubility of any volatiles trapped along the melt interfaces (cf. Zhang, 1999). As an explicit applied example, we considered the 2008 eruption of Volcán Chaitén (Chile), for which fractures have been shown to play a key role in the outgassing mechanisms (Castro et al., 2012). At the eruptive temperature of 825 °C, Castro and Dingwell (2009) constrained the melt viscosity at storage conditions and the conditions of shallow ascent to be in the range of 10^6–10^8 Pa·s. Using the model presented herein, this results in a fracture healing onset time scale of $10^{-3} \le \lambda_c \le 10^{-1}$ s. Then, applying the power-law model in Figure 2, we find the time for complete fracture healing is on the order of 10^0–10^2 s. The key finding here is that this range of time scales is the same as those over which strength recovers toward that of intact glass. Over times much shorter than these healing and strength recovery time scales, the fracture is weak and prone to repeated rupture. Indeed, Figure 3 shows that even after thorough healing, trapped bubbles remain, which may suppress total strength recovery and permanently weaken the relict fracture (even low porosities can weaken silicate melts relative to a nonporous melt of the same composition; Vasseur et al., 2013).

As silicic magmas approach the surface and extrude as domes, they are often highly degassed (Castro et al., 2012), which, using the viscosity model of Hess and Dingwell (1996), results in viscosities that increase to 10^9 Pa·s (see the Data Repository for this calculation). In turn, this increases the fracture healing time scales to 10^3–10^4 s. This shows that while fractures may rapidly heal during ascent (Gonnermann and Manga, 2003), once silicic magma is degassed, in-dome healing is far less efficient, and so the fractures may remain weak over long time scales and repetitively re-open during dome extrusion. This would imply that open-system outgassing can be maintained for long periods in the upper conduit and dome. Our model also demonstrates that postemplacement cooling will extend fracture healing time scales significantly. Other examples of eruptions that have produced glassy rhyolites are good candidates for applications of the work presented here (e.g., Tuffen et al., 2003; Tuffen and Dingwell, 2005; Cabrera et al., 2011).

There is abundant textural evidence for healed or partially healed fractures in volcanic rocks produced from silicic eruptions (e.g., Tuffen and Dingwell, 2005; Cabrera et al., 2011). Some examples may be complicated by the presence of particulate material (fragments of magma and/or country rock) trapped within fracture networks (Tuffen et al., 2003), which may obstruct fracture closure. In these cases, total healing is controlled by sintering of partly crystalline particles (Kendrick et al., 2016) or glass fragments (Vasseur et al., 2013), and it occurs over time scales

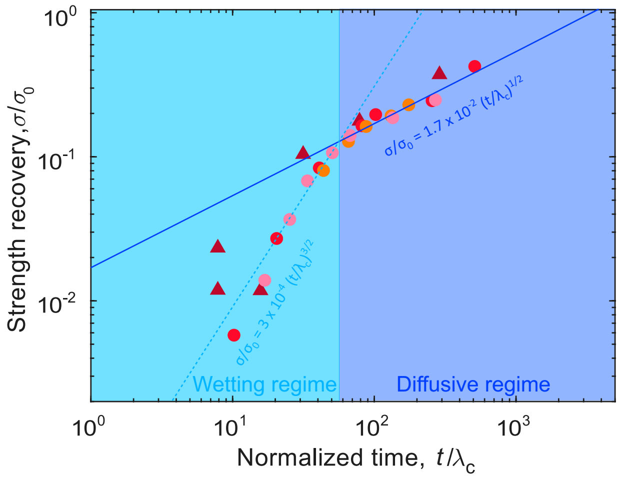

Figure 2. Kinetics of fracture healing shown by strength recovery against normalized time t/λ_c (λ_c is onset time), where we take $\lambda_c = 10\tau$ (τ is relaxation time) as the normalization value (Fig. 1C). Following relaxation of compressive stress, fracture healing is controlled by wetting of interfaces by diffusion, and then by diffusive mass exchange only, which have characteristic slopes of 3/2 and 1/2, respectively. Best-fit power-law equations for these regimes are shown on figure, which were used in the text to calculate total healing time; for example, of 2008 eruption of Volcán Chaitén (Chile). Uncertainties on σ/σ_0 (σ is strength of the partially healed fractured sample; σ_0 is tensile strength) are smaller than data points.

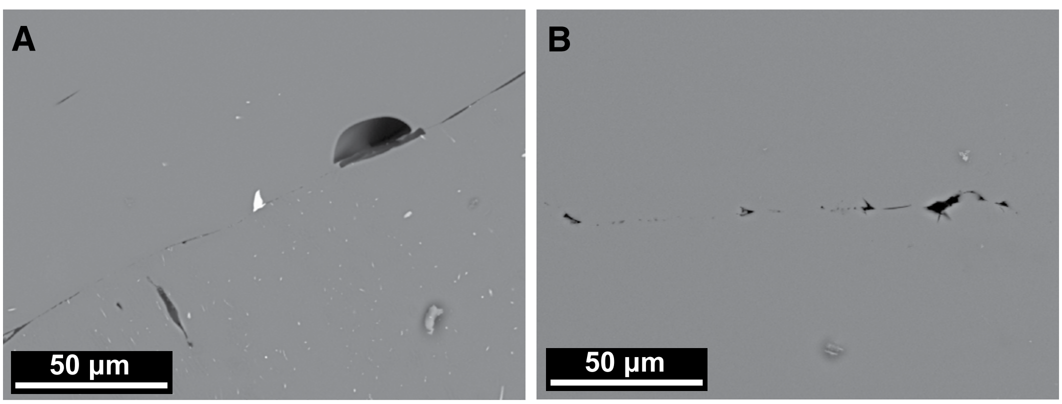

Figure 3. A: Backscattered-electron (BSE) image of a vesicle trapped in a fracture plane in an obsidian sample from Long Valley Caldera, California, USA, which indicates relict evidence for fracture healing. B: BSE image of experimentally healed sample, showing a similar texture to naturally healed obsidian.

proportional to the properties of the fracture fill at eruptive temperatures (Wadsworth et al., 2014) and the pressure acting on the fracture (Ryan et al., 2018), resulting in densification that reduces the system permeability (Kendrick et al., 2016; Wadsworth et al., 2016, 2017; Ryan et al., 2018). We note that in the other end-member system of particle-free fractures constrained here, the permeability does not decay as slowly as with particle-bearing fractures. Instead, the gas permeability of the fracture can drop rapidly as the planar fracture seals shut, unimpeded by particles, and this healing scales with the strength recovery.

During ascent, viscosity can vary spatially across a conduit (Costa and Macedonio, 2003; Mastin, 2005), thus affecting the occurrence of fracture healing processes. Such variations may lead to variably efficient permeable pathway closure and strength recovery in marginal shear zones, thus affecting outgassing and pressure distribution in volcanic conduits.

CONCLUSIONS

Conducting novel fracture healing experiments on silicate liquids at magmatic viscosities, we demonstrated that healing initiates after a time scale proportional to the relaxation time scale (and therefore viscosity). Beyond this point, healing begins via wetting of the surface, which transitions into a purely diffusional regime. During this process, soluble volatiles may get trapped as a trail of bubbles, which may impact the strength recovery magnitude. The findings suggest that at volcanoes, fracture healing, even when partially complete, may be an efficient process, and we posit that this may contribute to eruptive time scales or cyclicity.

ACKNOWLEDGMENTS

We acknowledge support from the European Research Council (ERC) Starting Grant on Strain Localization in Magmas (SLiM, no. 306488). J. Kendrick was funded by an Early Career Fellowship of the Leverhulme Trust (ECF 2016–325). We thank Instron® and Severn Thermal Solutions Limited for the joint development of the experimental apparatus. We are grateful to A. Ryan, H. Tuffen, L. Kennedy, M. Nakamura, and R. Weinberg for constructive reviews, and to D. Brown for editorial handling.

REFERENCES CITED

Berlo, K., Tuffen, H., Smith, V.C., Castro, J.M., Pyle, D.M., Mather, T.A., and Geraki, K., 2013, Element variations in rhyolitic magma resulting from gas transport: Geochimica et Cosmochimica Acta, v. 121, p. 436–451, https://doi.org/10.1016/j.gca.2013.07.032.

Cabrera, A., Weinberg, R.F., Wright, H.M.N., Zlotnik, S., and Cas, R.A.F., 2011, Melt fracturing and healing: A mechanism for degassing and origin of silicic obsidian: Geology, v. 39, p. 67–70, https://doi.org/10.1130/G31355.1.

Castro, J.M., and Dingwell, D.B., 2009, Rapid ascent of rhyolitic magma at Chaitén volcano, Chile: Nature, v. 461, no. 7265, p. 780–783, https://doi.org/10.1038/nature08458.

Castro, J.M., Cordonnier, B., Tuffen, H., Tobin, M.J., Puskar, L., Martin, M.C., and Bechtel, H.A., 2012, The role of melt-fracture degassing in defusing explosive rhyolite eruptions at volcán Chaitén: Earth and Planetary Science Letters, v. 333–334, p. 63–69, https://doi.org/10.1016/j.epsl.2012.04.024.

Castro, J.M., Bindeman, I.N., Tuffen, H., and Ian Schipper, C., 2014, Explosive origin of silicic lava: Textural and δD H_2O evidence for pyroclastic degassing during rhyolite effusion: Earth and Planetary Science Letters, v. 405, p. 52–61, https://doi.org/10.1016/j.epsl.2014.08.012.

Costa, A., and Macedonio, G., 2003, Viscous heating in fluids with temperature-dependent viscosity: Implications for magma flows: Nonlinear Processes in Geophysics, v. 10, p. 545–555, https://doi.org/10.5194/npg-10-545-2003.

Dingwell, D., and Webb, S.L., 1989, Structural relaxation in silicate melts and non-Newtonian melt rheology in geologic processes: Physics and Chemistry of Minerals, v. 16, p. 508–516, https://doi.org/10.1007/BF00197020.

Edmonds, M., Oppenheimer, C., Pyle, D.M., Herd, R.A., and Thompson, G., 2003, SO_2 emissions from Soufrière Hills Volcano and their relationship to conduit permeability, hydrothermal interaction and degassing regime: Journal of Volcanology and Geothermal Research, v. 124, p. 23–43, https://doi.org/10.1016/S0377-0273(03)00041-6.

Gardner, J.E., Llewellin, E.W., Watkins, J.M., and Befus, K.S., 2017, Formation of obsidian pyroclasts by sintering of ash particles in the volcanic conduit: Earth and Planetary Science Letters, v. 459, p. 252–263, https://doi.org/10.1016/j.epsl.2016.11.037.

Gonnermann, H.M., and Manga, M., 2003, Explosive volcanism may not be an inevitable consequence of magma fragmentation: Nature, v. 426, p. 432–435, https://doi.org/10.1038/nature02138.

Goto, A., 1999, A new model for volcanic earthquake at Unzen Volcano: Melt rupture model: Geophysical Research Letters, v. 26, p. 2541–2544, https://doi.org/10.1029/1999GL900569.

Hess, K.U., and Dingwell, D.B., 1996, Viscosities of hydrous leucogranitic melts: A non-Arrhenian model: The American Mineralogist, v. 81, p. 1297–1300, https://doi.org/10.2138/am-1996-9-1031.

ISRM (International Society for Rock Mechanics and Rock Engineering), 1978, Suggested methods for determining tensile strength of rock materials: International Journal of Rock Mechanics and Mining Sciences & Geomechanics Abstracts, v. 15, p. 4.

Kendrick, J.E., Lavallée, Y., Varley, N.R., Wadsworth, F.B., Lamb, O.D., and Vasseur, J., 2016, Blowing off steam: Tuffisite formation as a regulator for lava dome eruptions: Frontiers of Earth Science, v. 4, p. 41, https://doi.org/10.3389/feart.2016.00041.

Kolzenburg, S., Heap, M.J., Lavallée, Y., Russell, J.K., Meredith, P.G., and Dingwell, D.B., 2012, Strength and permeability recovery of tuffisite-bearing andesite: Solid Earth, v. 3, p. 191–198, https://doi.org/10.5194/se-3-191-2012.

Mastin, L.G., 2005, The controlling effect of viscous dissipation on magma flow in silicic conduits: Journal of Volcanology and Geothermal Research, v. 143, p. 17–28, https://doi.org/10.1016/j.jvolgeores.2004.09.008.

Neuberg, J.W., Tuffen, H., Collier, L., Green, D., Powell, T., and Dingwell, D.B., 2006, The trigger of low-frequency earthquakes on Montserrat: Journal of Volcanology and Geothermal Research, v. 153, p. 37–50, https://doi.org/10.1016/j.jvolgeores.2005.08.008.

Ryan, A.G., Friedlander, E.A., Russell, J.K., Heap, M.J., and Kennedy, L.A., 2018, Hot pressing in conduit faults during lava dome extrusion: Insights from Mount St. Helens 2004–2008: Earth and Planetary Science Letters, v. 482, p. 171–180, https://doi.org/10.1016/j.epsl.2017.11.010.

Tuffen, H., and Dingwell, D., 2005, Fault textures in volcanic conduits: Evidence for seismic trigger mechanisms during silicic eruptions: Bulletin of Volcanology, v. 67, p. 370–387, https://doi.org/10.1007/s00445-004-0383-5.

Tuffen, H., Dingwell, D.B., and Pinkerton, H., 2003, Repeated fracture and healing of silicic magma generate flow banding and earthquakes?: Geology, v. 31, p. 1089–1092, https://doi.org/10.1130/G19777.1.

Vasseur, J., Wadsworth, F.B., Lavallée, Y., Hess, K.-U., and Dingwell, D.B., 2013, Volcanic sintering: Timescales of viscous densification and strength recovery: Geophysical Research Letters, v. 40, p. 5658–5664, https://doi.org/10.1002/2013GL058105.

Wadsworth, F.B., Vasseur, J., von Aulock, F.W., Hess, K.-U., Scheu, B., Lavallée, Y., and Dingwell, D.B., 2014, Non-isothermal viscous sintering of volcanic ash: Journal of Geophysical Research–Solid Earth, v. 119, p. 8792–8804, https://doi.org/10.1002/2014JB011453.

Wadsworth, F.B., Vasseur, J., Scheu, B., Kendrick, J.E., Lavallée, Y., and Dingwell, D.B., 2016, Universal scaling of fluid permeability during volcanic welding and sediment diagenesis: Geology, v. 44, p. 219–222, https://doi.org/10.1130/G37559.1.

Wadsworth, F.B., et al., 2017, Topological inversions in coalescing granular media control fluid-flow regimes: Physical Review E, v. 96, p. 033113, https://doi.org/10.1103/PhysRevE.96.033113.

Wool, R., and O'Connor, K., 1981, A theory of crack healing in polymers: Journal of Applied Physics, v. 52, p. 5953–5963, https://doi.org/10.1063/1.328526.

Yoshimura, S., and Nakamura, M., 2010, Fracture healing in a magma: An experimental approach and implications for volcanic seismicity and degassing: Journal of Geophysical Research–Solid Earth, v. 115, B09209, https://doi.org/10.1029/2009JB000834.

Zhang, Y., 1999, H_2O in rhyolitic glasses and melts: Measurement, speciation, solubility, and diffusion: Reviews of Geophysics, v. 37, p. 493–516, https://doi.org/10.1029/1999RG900012.

Printed in USA